CrossMark

TECHNICAL ARTICLE

Crystal structure of ziprasidone hydrochloride monohydrate, $C_{21}H_{22}Cl_2N_4OS(H_2O)$

James A. Kaduk,[1,a] Kai Zhong,[2] Amy M. Gindhart,[2] and Thomas N. Blanton[2]
[1]*Illinois Institute of Technology, 3101 S. Dearborn St., Chicago, Illinois 60616*
[2]*ICDD, 12 Campus Blvd., Newtown Square, Pennsylvania 19073-3273*

(Received 30 December 2014; accepted 31 March 2015)

The crystal structure of ziprasidone hydrochloride monohydrate has been solved and refined using synchrotron X-ray powder diffraction data, and optimized using density functional techniques. Ziprasidone hydrochloride monohydrate crystallizes in space group *P*-1 (#2) with $a = 7.250\ 10(3)$, $b = 10.986\ 66(8)$, $c = 14.071\ 87(14)$ Å, $\alpha = 83.4310(4)$, $\beta = 80.5931(6)$, $\gamma = 87.1437(6)°$, $V = 1098.00(1)$ Å^3, and $Z = 2$. The ziprasidone conformation in the solid state is very close to the minimum energy conformation. The positively-charged nitrogen in the ziprasidone makes a strong hydrogen bond with the chloride anion. The water molecule makes two weaker bonds to the chloride, and acts as an acceptor in an N–H···O hydrogen bond. The powder pattern is included in the Powder Diffraction File™ as entry 00-064-1492. © *2015 International Centre for Diffraction Data*.
[doi:10.1017/S0885715615000305]

Key words: ziprasidone, Geodon, Zeldox, powder diffraction, Rietveld refinement, density functional theory

I. INTRODUCTION

Ziprasidone hydrochloride monohydrate (marketed as Geodon or Zeldox) is an FDA-approved oral formulation of ziprasidone. It acts as an atypical antipsychotic used for the treatment of schizophrenia and bipolar disorder (Greenberg and Citrome, 2007). The systematic name (CAS registry number 138982-67-9) is 5-[2-[4-(1,2-benzisothiazol-3-yl) piperazin-1-yl]ethyl]-6-chloroindolin-2-one hydrochloride hydrate. A two-dimensional molecular structure diagram is shown in Figure 1.

The presence of high-quality reference powder patterns in the Powder Diffraction File (PDF; ICDD, 2014) is important for phase identification, particularly by pharmaceutical, forensic, and law enforcement scientists. The crystal structures of a significant fraction of the largest dollar volume pharmaceuticals have not been published, and thus calculated powder patterns are not present in the PDF-4 databases. Sometimes experimental patterns are reported, but they are generally of low quality. This structure is a result of collaboration among ICDD, Illinois Institute of Technology (IIT), Poly Crystallography Inc., and Argonne National Laboratory to measure high-quality synchrotron powder patterns of commercial pharmaceutical ingredients, include these reference patterns in the PDF, and determine the crystal structures of these active pharmaceutical ingredients (APIs).

Even when the crystal structure of an API is reported, the single crystal structure was often determined at low temperature. Most powder measurements are performed at ambient conditions. Thermal expansion (often anisotropic) means that the peak positions calculated from a low-temperature single-crystal structure often differ significantly from those measured at ambient conditions. These peak shifts can result in failure of default search/match algorithms to identify a phase, even when it is present in the sample. High-quality reference patterns measured at ambient conditions are thus critical for easy identification of APIs using standard powder diffraction practices.

II. EXPERIMENTAL

Ziprasidone hydrochloride monohydrate was purchased from the United States Pharmacopeia (USP) (Lot FOJ028), and was used as-received. The white powder was packed into a 1.5 mm diameter Kapton capillary, and rotated during the measurement at ~50 cycles s^{-1}. The powder pattern was measured at 295 K at beam line 11-BM (Lee *et al.*, 2008; Wang *et al.*, 2008) of the Advanced Photon Source at the Argonne National Laboratory using a wavelength of 0.413 914 Å from 0.5° to 50° 2θ with a step size of 0.001° and a counting time of 0.1 s step^{-1}. The pattern was indexed on a primitive triclinic unit cell having $a = 7.2494$, $b = 10.9937$, $c = 14.0771$ Å, $\alpha = 83.437$, $\beta = 80.602$, $\gamma = 87.158°$, $V = 1099.06$ Å^3, and $Z = 2$ using N-TREOR incorporated into EXPO2013 (Altomare *et al.*, 2013). A search of this cell in the Cambridge Structural Database (Allen, 2002) yielded 73 hits, but no crystal structure for ziprasidone hydrochloride monohydrate. The space group was assumed to be *P*-1, which was confirmed by successful solution and refinement of the structure.

A ziprasidone cation was built and its conformation optimized using Spartan '14 (Wavefunction, 2013), and saved as a mol2 file. This file was converted into a Fenske–Hall *Z*-matrix file using OpenBabel (O'Boyle *et al.*, 2011). This molecule, a chlorine atom, and an oxygen atom (for the water molecule)

[a]Author to whom correspondence should be addressed. Electronic mail: kaduk@polycrystallography.com

https://doi.org/10.1017/S0885715615000305 Published online by Cambridge University Press

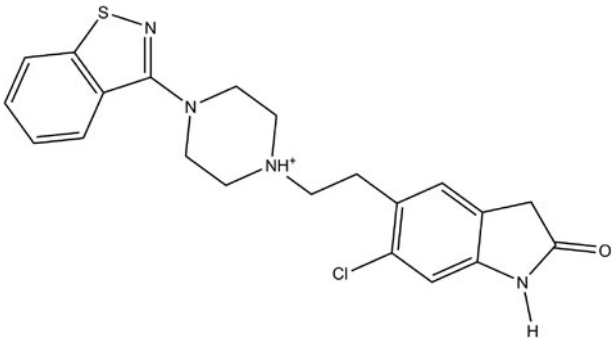


Figure 1. The molecular structure of the ziprasidone cation.

were used to solve the structure with FOX (Favre-Nicolin and Černý, 2002). The maximum $\sin\theta/\lambda$ used in the solution was 0.40 $Å^{-1}$. The oxygen atom moved too close to the Cl, and was removed from the initial refinements. A reasonable oxygen was the highest peak in a difference Fourier map, and the oxygen O51 was added at that position. Initial positions of the active hydrogens were deduced by analysis of potential hydrogen-bonding patterns.

Rietveld refinement was carried out using GSAS (Larson and Von Dreele, 2004). Only the 1.5°–25° portion of the pattern ($d_{min} = 0.96$ Å) was included in the refinement. All non-hydrogen bond distances and angles were subjected to restraints, based on a Mercury/Mogul Geometry Check (Bruno *et al.*, 2004; Sykes *et al.*, 2011) of the molecule. The Mogul average and standard deviation for each quantity were used as the restraint parameters. The C4–C9 and C34–C39 aromatic rings were subjected to a planar restraint with a standard deviation of 0.01 Å. The restraints contributed 4.05% to the final χ^2. Isotropic displacement coefficients were refined, grouped by chemical similarity. The hydrogen atoms were included in calculated positions, which were recalculated during the refinement. The U_{iso} of each hydrogen atom was constrained to be 1.3 times that of the heavy atom to which it is attached. The peak profiles were described using profile function number 4 (Thompson *et al.*, 1987; Finger *et al.*, 1994), which includes the Stephens (1999) anisotropic strain broadening model. The background was modeled using a six-term shifted Chebyshev polynomial. The final refinement of 104 variables using 23 576 observations yielded the residuals $R_{wp} = 0.067$, $R_p = 0.054$, and $\chi^2 = 1.796$. The largest peak (2.17 Å from H48) and hole (1.24 Å from C29) in the difference Fourier map were 0.30 and −0.31 e ($Å^{-3}$), respectively. The Rietveld plot is included as Figure 2. The largest errors are subtle mis-fits in the shapes of the low-angle peaks, and may reflect subtle changes in the specimen during the measurement.

A density functional geometry optimization (fixed experimental unit cell) was carried out using CRYSTAL09 (Dovesi *et al.*, 2005). The basis sets for the H, C, N, and O atoms were those of Gatti *et al.* (1994), the basis set for S was that of Lichanot *et al.* (1993), and the basis set for Cl was that of Apra *et al.* (1993). The calculation used eight k-points and the B3LYP functional. Re-starting the Rietveld refinement from the density functional theory (DFT)-optimized structure yielded residuals $R_{wp} = 0.069$ and $\chi^2 = 1.961$. The re-refined structure was essentially identical to the Rieitveld refinement prior to DFT, with a root-mean-square displacement of the non-hydrogen atoms of 0.06 Å.

III. RESULTS AND DISCUSSION

The refined atom coordinates of ziprasidone hydrochloride monohydrate are reported in Table I, and the coordinates from the DFT optimization in Table II. The root-mean-square deviation of the non-hydrogen atoms is 0.12 Å, and the maximum deviation is 0.31 Å, at O43 (Figure 3). The discussion

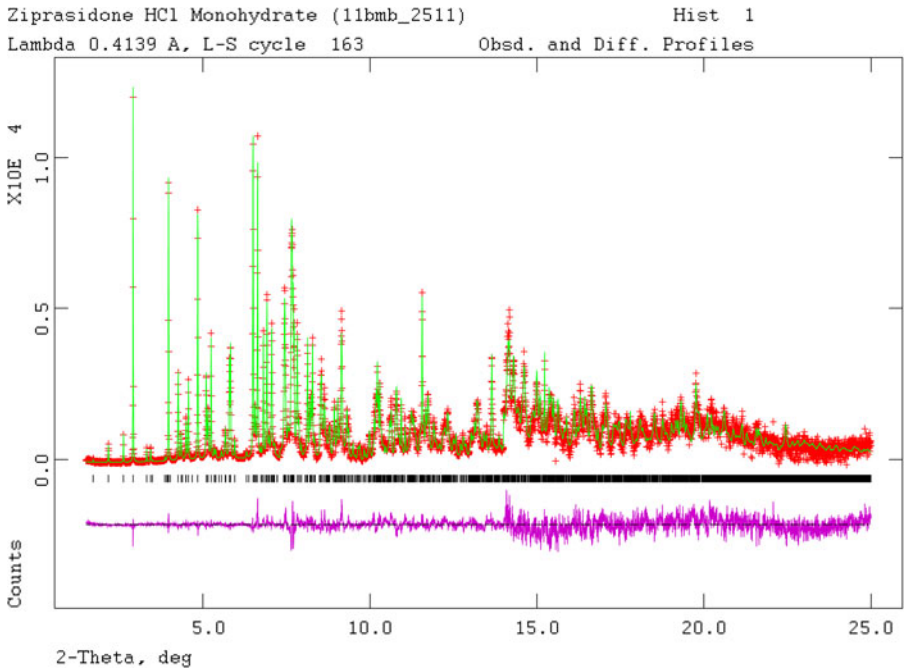


Figure 2. (Color online) The Rietveld plot for the refinement of ziprasidone hydrochloride monohydrate. The red crosses represent the observed data points, and the green line is the calculated pattern. The magenta curve is the difference pattern, plotted at the same vertical scales as the other patterns. The vertical scale has been multiplied by a factor of 5 for $2\theta > 7.3°$, and by a factor of 20 for $2\theta > 14.0°$.

https://doi.org/10.1017/S0885715615000305 Published online by Cambridge University Press

TABLE I. Rietveld refined crystal structure of ziprasidone hydrochloride monohydrate.

Crystal data	
$C_{21}H_{24}Cl_2N_4O_2S$	$\beta = 80.5931\ (6)^\circ$
$M_r = 467.41$	$\gamma = 87.1437\ (6)^\circ$
Triclinic, *P*-1	$V = 1098.00\ (1)$ Å^3
$a = 7.250\ 10\ (3)$ Å	$Z = 2$
$b = 10.986\ 66\ (8)$ Å	Synchrotron radiation, $\lambda = 0.413\ 914$ Å
$c = 14.071\ 87\ (14)$ Å	1.5 mm Kapton capillary
$\alpha = 83.4310\ (4)^\circ$	

Refinement	
Least-squares matrix: full	23 576 data points
$R_p = 0.054$	Profile function: CW Profile function number 4 with 27 terms Pseudovoigt profile coefficients as parameterized in Thompson *et al.* (1987). Asymmetry correction of Finger *et al.* (1994). Microstrain broadening by Stephens (1999). #1(GU) = 1.163 #2(GV) = −0.126 #3(GW) = 0.063 #4(GP) = 0.000 #5(LX) = 0.173 #6(ptec) = 0.00 #7(trns) = 0.00 #8(shft) = 0.0000 #9 (sfec) = 0.00 #10(S/L) = 0.0011 #11(H/L) = 0.0011 #12(eta) = 0.8000 Peak tails are ignored where the intensity is below 0.0020 times the peak Aniso. broadening axis 0.0 0.0 1.0
$R_{wp} = 0.067$	104 parameters
$R_{exp} = 0.051$	77 restraints
$R(F^2) = 0.082\ 26$	$(\Delta/\sigma)_{max} = 0.03$
$\chi^2 = 1.796$	Background function: GSAS Background function number 1 with six terms. Shifted Chebyshev function of first kind 1: 201.094 2: −41.0040 3: 24.0256 4: −24.5371 5: 6.666 32 6: −10.4117

Fractional atomic coordinates and isotropic displacement parameters (Å^2)

	x	*y*	*Z*	U_{iso} (Å^2)
S1	0.2511 (5)	−0.2599 (3)	0.4246 (2)	0.0636 (10)
N2	0.2824 (9)	−0.1507 (6)	0.4943 (5)	0.0636 (10)
C3	0.1513 (11)	−0.1492 (8)	0.5676 (5)	0.0636 (10)
C4	−0.0216 (9)	−0.2179 (7)	0.5627 (5)	0.0636 (10)
C5	−0.2013 (10)	−0.2123 (7)	0.6126 (5)	0.0636 (10)
C6	−0.3162 (10)	−0.2952 (7)	0.5914 (5)	0.0636 (10)
C7	−0.2798 (11)	−0.3750 (7)	0.5232 (6)	0.0636 (10)
C8	−0.1066 (11)	−0.3765 (7)	0.4719 (5)	0.0636 (10)
C9	0.0272 (9)	−0.2986 (6)	0.4895 (5)	0.0636 (10)
H10	−0.223 09	−0.158 22	0.673 41	0.0827 (12)
H11	−0.456 85	−0.294 45	0.637 38	0.0827 (12)
H12	−0.379 55	−0.429 18	0.506 38	0.0827 (12)
H13	−0.066 48	−0.422 12	0.4018	0.0827 (12)
N14	0.1506 (9)	−0.0651 (7)	0.6352 (5)	0.0272 (13)
C15	0.1282 (11)	−0.1228 (6)	0.7358 (6)	0.0272 (13)
C16	0.0748 (11)	−0.0180 (7)	0.7977 (5)	0.0272 (13)
N17	0.2317 (9)	0.0690 (5)	0.7731 (5)	0.0272 (13)
C18	0.2698 (12)	0.1244 (6)	0.6688 (7)	0.0272 (13)
C19	0.3001 (12)	0.0179 (8)	0.6125 (5)	0.0272 (13)
H20	0.016 73	−0.1784	0.749 46	0.0353 (16)
H21	0.260 17	−0.1717	0.7493	0.0353 (16)
H22	−0.035 47	0.033 22	0.791 67	0.0353 (16)
H23	0.0869	−0.056 08	0.8772	0.0353 (16)
H24	0.151 19	0.173 99	0.664 32	0.0353 (16)
H25	0.395 26	0.183 31	0.662 99	0.0353 (16)
H26	0.450 32	−0.029 41	0.620 42	0.0353 (16)
H27	0.329 86	0.059 74	0.536 98	0.0353 (16)
C28	0.1988 (12)	0.1717 (7)	0.8414 (6)	0.037 (3)
C29	0.3591 (10)	0.2562 (7)	0.8513 (5)	0.037 (3)
H30	0.096 89	0.232 32	0.817 13	0.048 (3)
H31	0.146 72	0.131 14	0.918 31	0.048 (3)
H32	0.475 55	0.188 63	0.889 46	0.048 (3)
H33	0.451 78	0.275 38	0.779 64	0.048 (3)
C34	0.3078 (9)	0.3612 (5)	0.9065 (4)	0.0136 (7)
C35	0.2968 (9)	0.4723 (6)	0.8533 (5)	0.0136 (7)
C36	0.2569 (10)	0.5788 (6)	0.9046 (5)	0.0136 (7)
C37	0.2392 (10)	0.5547 (5)	1.0077 (4)	0.0136 (7)
C38	0.2504 (10)	0.4354 (5)	1.0597 (4)	0.0136 (7)

Continued

https://doi.org/10.1017/S0885715615000305 Published online by Cambridge University Press

TABLE I. Continued

Crystal data				
C39	0.2905 (9)	0.3370 (5)	1.0060 (5)	0.0136 (7)
N40	0.2005 (9)	0.6413 (4)	1.0771 (4)	0.0136 (7)
C41	0.1982 (11)	0.5819 (5)	1.1719 (4)	0.0136 (7)
C42	0.2194 (11)	0.4425 (6)	1.1680 (5)	0.0136 (7)
O43	0.1640 (7)	0.6382 (4)	1.2459 (4)	0.0136 (7)
H44	0.270 89	0.672 27	0.868 94	0.0177 (10)
H45	0.292 26	0.253 28	1.046 47	0.0177 (10)
H46	0.298 49	0.419 32	1.208 46	0.0177 (10)
H47	0.060 16	0.415 17	1.198 93	0.0177 (10)
H48	0.202 49	0.743 29	1.0561	0.0177 (10)
Cl49	0.3156 (4)	0.5085 (3)	0.7358 (2)	0.0666 (14)
Cl50	0.5798 (4)	0.9292 (2)	0.841 77 (18)	0.0441 (12)
O51	0.2599 (8)	0.9058 (5)	1.0232 (4)	0.048 (2)
H52	0.371 25	0.026 69	0.798 21	0.0353 (16)
H53	0.368 77	0.900 49	0.968 74	0.062 (3)
H54	0.263 87	0.953 68	1.060 07	0.062 (3)

TABLE II. DFT-optimized (CRYSTAL09) structure of ziprasidone hydrochloride monohydrate.

Crystal data	
$C_{21}H_{24}Cl_2N_4O_2S$	$\beta = 80.5931°$
$M_r = 467.41$	$\gamma = 87.1437°$
Triclinic, *P*-1	$V = 1098.00$ Å^3
$a = 7.2501$ Å	$Z = 2$
$b = 10.9867$ Å	$\lambda = 0.413\,914$ Å
$c = 14.0719$ Å	
$\alpha = 83.4310°$	

Fractional atomic coordinates and isotropic displacement parameters (Å^2)

	x	*y*	*z*	U_{iso}
S1	0.257 16	−0.259 37	0.418 50	0.064
N2	0.301 68	−0.158 48	0.496 30	0.064
C3	0.156 58	−0.146 27	0.563 75	0.064
C4	−0.005 47	−0.217 54	0.560 25	0.064
C5	−0.184 87	−0.218 01	0.616 48	0.064
C6	−0.317 08	−0.294 17	0.596 01	0.064
C7	−0.274 18	−0.369 83	0.520 58	0.064
C8	−0.099 94	−0.368 01	0.462 35	0.064
C9	0.032 33	−0.290 13	0.482 53	0.064
H10	−0.223 09	−0.158 22	0.673 41	0.083
H11	−0.456 85	−0.294 45	0.637 38	0.083
H12	−0.379 55	−0.429 18	0.506 38	0.083
H13	−0.066 48	−0.422 12	0.401 80	0.083
N14	0.159 70	−0.064 05	0.632 54	0.027
C15	0.134 00	−0.117 47	0.734 09	0.027
N17	0.248 88	0.072 87	0.782 02	0.027
C18	0.278 58	0.121 76	0.676 53	0.027
C19	0.316 52	0.018 87	0.611 88	0.027
C16	0.094 36	−0.017 62	0.801 76	0.027
H20	0.016 73	−0.178 40	0.749 46	0.035
H21	0.260 17	−0.171 70	0.749 30	0.035
H22	−0.035 47	0.033 22	0.791 67	0.035
H23	0.086 90	−0.056 08	0.877 20	0.035
H24	0.151 19	0.173 99	0.664 32	0.035
H25	0.395 26	0.183 31	0.662 99	0.035
H26	0.450 32	−0.029 41	0.620 42	0.035
H27	0.329 86	0.059 74	0.536 98	0.035
C28	0.205 11	0.174 34	0.846 69	0.037

Continued

https://doi.org/10.1017/S0885715615000305 Published online by Cambridge University Press

TABLE II. Continued

Crystal data				
C29	0.377 45	0.246 98	0.851 99	0.037
H30	0.096 89	0.232 32	0.817 13	0.048
H31	0.146 72	0.131 14	0.918 31	0.048
H32	0.475 55	0.188 63	0.889 46	0.048
H33	0.451 78	0.275 38	0.779 64	0.048
C34	0.322 97	0.358 29	0.905 66	0.014
C35	0.309 92	0.477 05	0.859 53	0.014
C36	0.270 97	0.581 55	0.908 11	0.014
C37	0.237 87	0.562 96	1.008 58	0.014
C38	0.240 12	0.444 84	1.058 71	0.014
C39	0.284 40	0.344 27	1.007 81	0.014
N40	0.196 82	0.650 01	1.074 41	0.014
C41	0.169 31	0.595 89	1.168 54	0.014
C42	0.192 33	0.457 02	1.165 38	0.014
O43	0.129 35	0.651 34	1.240 42	0.014
H44	0.270 89	0.672 27	0.868 94	0.018
H45	0.292 26	0.253 28	1.046 47	0.018
H46	0.298 49	0.419 32	1.208 46	0.018
H47	0.060 16	0.415 17	1.198 93	0.018
H48	0.202 49	0.743 29	1.056 10	0.018
Cl49	0.342 40	0.501 77	0.727 84	0.067
Cl50	0.607 84	0.929 77	0.846 46	0.044
O51	0.246 00	0.902 37	1.009 99	0.048
H52	0.371 25	0.026 69	0.798 21	0.035
H53	0.368 77	0.900 49	0.968 74	0.062
H54	0.263 87	0.953 68	1.060 07	0.062

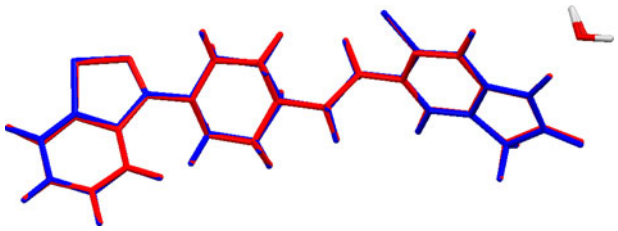


Figure 3. (Color online) Comparison of the refined and optimized structures of ziprasidone hydrochloride monohydrate. The Rietveld-refined structure is in red, and the DFT-optimized structure is colored blue.

of the geometry uses the DFT-optimized structure. The asymmetric unit (with atom numbering) is illustrated in Figure 4, and the crystal structure is presented in Figure 5.

Most bond distances, all angles, and all torsion angles fall within the normal ranges indicated by a Mercury Mogul Geometry Check. The S1–N2 distance of 1.721 Å (average = 1.672(9) Å, *Z*-score = 5.52), the S1–C9 distance of 1.757 Å (average = 1.722(15) Å, *Z*-score = 2.39), and the C35–Cl49 distance of 1.820 Å (average = 1.732(25) Å, *Z*-score = 3.53) are flagged as unusual. The effect of a change in heavy atom basis set on these optimized distances was not explored.

Both quantum mechanical (DFT/B3LYP functional/6-31G* basis set) and molecular mechanics (MMFF) conformational analyses using Spartan '14 suggest that the observed conformation in the solid state is very close (<5 kcal mol^{-1}) to the minimum energy conformation. An analysis of the contributions to the total crystal energy using the Forcite module of Materials Studio (Accelrys, 2013) suggests that the bond and torsion angle distortion contributions are small, while the angle distortion contributions are significant; the five-membered rings are probably strained. The crystal energy appears to be dominated by electrostatic contributions, which in this force-field-based analysis include hydrogen bonds. The

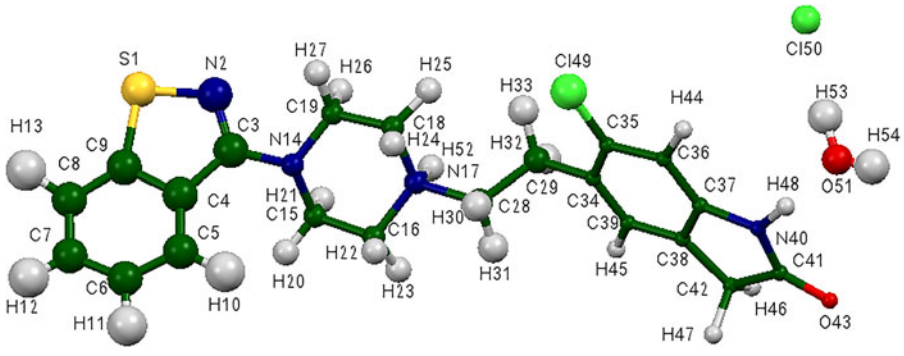


Figure 4. (Color online) The molecular structure of ziprasidone hydrochloride monohydrate, with the atom numbering. The atoms are represented by 50% probability spheroids.

https://doi.org/10.1017/S0885715615000305 Published online by Cambridge University Press

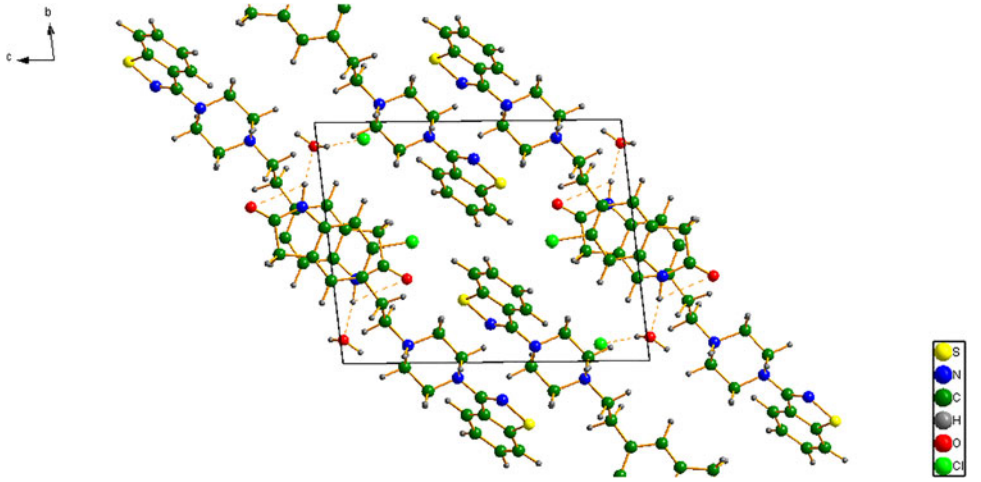


Figure 5. (Color online) The crystal structure of ziprasidone hydrochloride monohydrate, viewed down the *a*-axis. The hydrogen bonds are indicated by the dashed lines.

TABLE III. Hydrogen bonds in ziprasidone hydrochloride monohydrate.

D–H···A	D–H (Å)	H···A (Å)	D···A (Å)	D–H···A (°)	Overlap (*e*)
N17–H52···Cl50	1.045	2.138	3.179	174.1	0.075
O51–H53···Cl50	0.981	2.241	3.196	164.3	0.039
O51–H54···Cl50	0.979	2.267	3.217	163.3	0.034
H40–H48···O51	1.029	1.818	2.838	170.7	0.074
C28–H30···O43	1.091	2.229	3.320	178.6	0.030

hydrogen bonds are better analyzed using the results of the DFT calculation.

As expected, the positively-charged N17 makes a strong hydrogen bond with the chloride anion Cl50 (Table III). The water molecule O51 also makes two weaker hydrogen bonds to Cl50. The water molecule acts as a hydrogen bond acceptor from the ring group N40–H48. There is also a weaker C–H···O hydrogen bond to the carbonyl oxygen O43. Each of these hydrogen bonds is discrete. Two water molecules and two chloride anions form a *R*2,4(8) pattern (Etter, 1990; Bernstein *et al.*, 1995; Shields *et al.*, 2000). A significant contribution to the packing appears to be stacking of the flat portions of the molecule.

The Bravais–Friedel–Donnay–Harker (Bravais, 1866; Friedel, 1907; Donnay and Harker, 1937) morphology suggests that we might expect platy morphology for ziprasidone hydrochloride monohydrate, with {001} as the principal faces; no preferred orientation correction was necessary for this rotated capillary specimen. The powder pattern of ziprasidone hydrochloride monohydrate is included in the PDF as entry 00-064-1492.

SUPPLEMENTARY MATERIALS AND METHODS

The supplementary material for this article can be found at http://www.journals.cambridge.org/PDJ

ACKNOWLEDGMENTS

Use of the Advanced Photon Source at Argonne National Laboratory was supported by the US Department of Energy, Office of Science, Office of Basic Energy Sciences, under Contract No. DE-AC02-06CH11357. This work was partially supported by the International Centre for Diffraction Data. We thank Lynn Ribaud for his assistance in data collection.

Accelrys (**2013**). *Materials Studio 7.0* (Accelrys Software Inc., San Diego, CA).

Allen, F. H. (**2002**). "The Cambridge Structural Database: a quarter of a million crystal structures and rising," Acta Crystallogr. Sect. B: Struct. Sci. **58**, 380–388.

Altomare, A., Cuocci, C., Giacovazzo, C., Moliterni, A., Rizzi, R., Corriero, N., and Falcicchio, A. (**2013**). "EXPO2013: a kit of tools for phasing crystal structures from powder data," J. Appl. Crystallogr. **46**, 1231–1235.

Apra, E., Causa, M., Prencipe, M., Dovesi, R., and Saunders, V. R. (**1993**). "On the structural properties of NaCl: an ab initio study of the B1-B2 phase transition," J. Phys.: Condens. Matter **5**(18), 2969–2976.

Bernstein, J., Davis, R. E., Shimoni, L., and Chang, N. L. (**1995**). "Patterns in hydrogen bonding: functionality and graph set analysis in crystals," Angew. Chem. Int. Ed. Engl. **34**(15), 1555–1573.

Bravais, A. (**1866**). *Etudes Cristallographiques* (Gauthier Villars, Paris).

Bruno, I. J., Cole, J. C., Kessler, M., Luo, J., Motherwell, W. D. S., Purkis, L. H., Smith, B. R., Taylor, R., Cooper, R. I., Harris, S. E., and Orpen, A. G. (**2004**). "Retrieval of crystallographically-derived molecular geometry information," J. Chem. Inf. Sci. **44**, 2133–2144.

Donnay, J. D. H. and Harker, D. (**1937**). "A new law of crystal morphology extending the law of Bravais," Amer. Mineral. **22**, 446–467.

Dovesi, R., Orlando, R., Civalleri, B., Roetti, C., Saunders, V. R., and Zicovich-Wilson, C. M. (**2005**). "CRYSTAL: a computational tool for the *ab initio* study of the electronic properties of crystals," Z. Kristallogr. **220**, 571–573.

Etter, M. C. (**1990**). "Encoding and decoding hydrogen-bond patterns of organic compounds," Acc. Chem. Res. **23**(4), 120–126.

Favre-Nicolin, V. and Černý, R. (**2002**). "FOX, Free Objects for crystallography: a modular approach to ab initio structure determination from powder diffraction," J. Appl. Crystallogr. **35**, 734–743.

Finger, L. W., Cox, D. E., and Jephcoat, A. P. (**1994**). "A correction for powder diffraction peak asymmetry due to axial divergence," J. Appl. Crystallogr. **27**(6), 892–900.

https://doi.org/10.1017/S0885715615000305 Published online by Cambridge University Press

Friedel, G. (**1907**). "Etudes sur la loi de Bravais," Bull. Soc. Fr. Mineral. **30**, 326–455.

Gatti, C., Saunders, V. R., and Roetti, C. (**1994**). "Crystal-field effects on the topological properties of the electron-density in molecular crystals - the case of urea," J. Chem. Phys. **101**, 10686–10696.

Greenberg, W. M. and Citrome, L. (**2007**). "Ziprasidone for schizophrenia and bipolar disorder: a review of the clinical trials," CNS Drug Rev. **13**(2), 137–177.

ICDD (**2014**), PDF-4+ 2014 (Database). edited by Dr. Soorya Kabekkodu, International Centre for Diffraction Data, Newtown Square, PA, USA.

Larson, A. C. and Von Dreele, R. B. (**2004**). "General structure analysis system, (GSAS)", Los Alamos National Laboratory Report LAUR 86–784.

Lee, P. L., Shu, D., Ramanathan, M., Preissner, C., Wang, J., Beno, M. A., Von Dreele, R. B., Ribaud, L., Kurtz, C., Antao, S. M., Jiao, X., and Toby, B. H. (**2008**). "A twelve-analyzer detector system for high-resolution powder diffraction," J. Synchroton Radiat. **15**(5), 427–432.

Lichanot, A., Apra, E. and Dovesi, R. (**1993**). "Quantum mechanical Hartree–Fock study of the elastic properties of Li_2S and Na_2S," Phys. Status Solidi B **177**, 157–163.

O'Boyle, N., Banck, M., James, C. A., Morley, C., Vandermeersch, T. and Hutchison, G. R. (**2011**). "Open Babel: an open chemical toolbox," J. Chem. Inf. **3**, 33.

Shields, G. P., Raithby, P. R., Allen, F. H., and Motherwell, W. S. (**2000**). "The assignment and validation of metal oxidation states in the Cambridge Structural Database," Acta Crystallogr. Sec. B: Struct. Sci. **56**(3), 455–465.

Stephens, P. W. (**1999**). "Phenomenological model of anisotropic peak broadening in powder diffraction," J. Appl. Crystallogr. **32**, 281–289.

Sykes, R. A., McCabe, P., Allen, F. H., Battle, G. M., Bruno, I. J., and Wood, P. A. (**2011**). "New software for statistical analysis of Cambridge Structural Database data," J. Appl. Crystallogr. **44**, 882–886.

Thompson, P., Cox, D. E., and Hastings, J. B. (**1987**). "Rietveld refinement of Debye-Scherrer synchrotron X-ray data from Al_2O_3," J. Appl. Crystallogr. **20**(2), 79–83.

Wang, J., Toby, B. H., Lee, P. L., Ribaud, L., Antao, S. M., Kurtz, C., Ramanathan, M., Von Dreele, R. B., and Beno, M. A. (**2008**). "A dedicated powder diffraction beamline at the Advanced Photon Source: commissioning and early operational results," Rev. Sci. Instrum. **79**, 085105.

Wavefunction, Inc. (**2013**). Spartan '14 Version 1.1.0, Wavefunction Inc., 18401 Von Karman Ave., Suite 370, Irvine CA 92612.

https://doi.org/10.1017/S0885715615000305 Published online by Cambridge University Press